



5-(Phenyl-pyrrolidin-1-yl-methyl)-pyrimidine-2,4,6-trione: A Novel Corrosion Inhibitor for Mild Steel in Acidic Medium

K.P. Annamalai,^{*a} P. Iniyavan,^b V. Ashok Kumar,^c M. Gopiraman^{*d} and D. Tamilvendan^c

^aCAS-Haixi Institutes, Fuzhou, China - 350002.

^bJawaharlal Nehru Centre for Advanced Scientific Research, Bengaluru - 560064, India.

^cDepartment of Chemistry, National Institute of Technology, Tiruchirappalli - 620015, Tamilnadu, India.

^dDepartment of Applied Bioscience, College of Life & Environment Science, Konkuk University, Seoul - 05029, South Korea.

*Corresponding author E-mail address: kpannamalai@outlook.com (K.P. Annamalai); gopiraman@konkuk.ac.kr (M.Gopiraman)

ISSN: 2582-6239



Publication details

Received: 03rd November 2019

Revised: 03rd December 2019

Accepted: 27th December 2019

Published: 02nd January 2020

Abstract: A new Mannich base, namely, 5-(phenyl-pyrrolidin-1-yl-methyl)-pyrimidine-2,4,6-trione (PPMPT), was successfully synthesized by simple green synthesis and the resultant PPMPT was used as corrosion inhibitor for mild steel in 1.0 M hydrochloric acid (HCl). The corrosion inhibition efficiency was studied by means of weight loss method and electrochemical techniques. The results demonstrated that 400 ppm of PPMPT has more than 95% inhibition efficiency against corrosion of mild steel in 1 M HCl. Calculated values of adsorption parameters such as ΔH_{ads} and ΔS_{ads} revealed a strong interaction between inhibitor molecules and mild steel surface in acidic medium. Negative value of ΔG_{ads} indicates spontaneous adsorption of PPMPT molecules on the surface of mild steel. To further potentiodynamic polarization and electrochemical impedance measurements were also carried out to evaluate the type of inhibitor and corrosion inhibition mechanism, respectively. Ultraviolet-visible spectroscopy (UV-Visible), Fourier-transform infrared spectroscopy (FT-IR), scanning electron microscope and energy dispersion spectroscopy (SEM-EDS) were also carried out to support the inhibition efficiency of the PPMPT.

Keywords: Corrosion inhibition; Mild steel; Electrochemical impedance; Mannich base; Adsorption

1. Introduction

Mild steel is one of the most strong and affordable materials that can be effectively used in preparing wide range of building construction materials, machinery parts, cookware, industrial pipelines, visually aesthetic metal gate and fencing.^[1,2] However, the mild steel can easily undergoes severe corrosion under acidic environment.^[3] Acid solutions such as hydrochloric acid (HCl) and sulphuric acid (H₂SO₄) are extensively used for industrial cleaning, oil well acidification and in the petrochemical processes.^[4] In particular, the HCl is often used in the pickling processes of metals and alloys. Hence, corrosion inhibitors are being used to prevent metals from the acid corrosion.^[5] Most of the well-known acid corrosion inhibitors are organic compounds containing nitrogen (N), sulphur (S) and oxygen (O) atoms.^[6] Generally, inhibition efficiency should increase in the following order: O < N < S < P. To date, several organic compounds with heteroatom showed excellent corrosion inhibition ability towards the mild steel corrosion by the adsorption inhibition molecules on the metal surface.^[7] Among them, N and O containing heterocyclic compounds are considered to be most effective corrosion inhibitors for mild steel. Recent studies show that the inhibition efficiency of organic compound containing heterocyclic N and O obviously increases with the number of aromatic systems and

the availability of electronegative atoms present in the molecules.^[8] The selection of the inhibitor is based on two considerations: first it could be synthesized conveniently from relatively cheap raw materials; secondly, it contains the electron cloud on the aromatic ring or, the electronegative atoms such as nitrogen and oxygen in the relatively long chain or bulky compounds. In addition, the bulky molecules could obviously cover the surface of mild steel more effectively.^[9]

Literature review reveals that most of the commercial formulations include carbonyls and amines as essential ingredients, and their condensation products of carbonyls and amines known as anils, gave higher inhibition efficiency than that for constituent carbonyls and amines.^[10] So far, a very few Mannich bases have been reported as effective acidic and vapour phase corrosion inhibitors.^[11,12] However, there is no report on phenyl-pyrrolo-pyrimidine derivative as a mild steel corrosion inhibitor in the literature. Herein, we prepared a new Mannich base, namely, 5-(Phenyl-pyrrolidin-1-yl-methyl)-pyrimidine-2,4,6-trione (PPMPT), via green synthesis. The resultant PPMPT was used as corrosion inhibitor for mild steel in HCl. Weight loss and electrochemical methods were used to study the inhibitive performance of the PPMPT. Adsorption parameters such as ΔH_{ads} , ΔS_{ads} and ΔG_{ads} were calculated. Ultraviolet-visible spectroscopy (UV-Visible), Fourier-transform

infrared spectroscopy (FT-IR), scanning electron microscope and energy dispersion spectroscopy (SEM-EDS) were also carried out to support the inhibition efficiency of the PPMPT.

2. Experimental Section

2.1. Materials and Methods

Mild steel specimens having composition of 0.10% C, 0.34% Mn, 0.08% P, and the remainder being Fe were used. 3cm × 2cm × 0.35cm plates were used for weight loss method and 3cm × 2cm with 0.35 cm long stem (isolated with araldite) were used for electrochemical impedance methods. They were polished mechanically using emery paper of Grade No. 220, 400, 600, 800 and 1200 and washed thoroughly with double distilled water and degreased with acetone before immerse in the acid solution. The aggressive solution of 1.0 M HCl has been prepared by dilution of AR grade hydrochloric acid.

2.2. Synthesis of Inhibitor

The Mannich base was synthesized by condensation reaction between barbituric acid 2.56g (0.02mol), pyrrolidine 1.62mL (0.02mol) and benzaldehyde 2.04mL (0.02mol), stirred at room temperature for 30 minutes. As obtained white precipitate obtained washed thoroughly with hot water to remove excess of barbituric acid. The formation of compound was checked by TLC. Anal. Found: C, 62.71; H, 5.96; N, 14.63. Calc. for C₁₅H₁₇N₃O₃: C, 62.65; H, 5.99; N, 14.68. IR (KBr disk), cm⁻¹; ν_{NH} 3391, ν_{C-H} 3005 ν_{C=O} 1704 and 1591, ν_{C-N-C} 1171. ¹H NMR data (in dimethylsulfoxide-d₆): δ 1.6 ppm (C(3-4)-H₂); δ 2.2 ppm (C(2-5)-H₂); δ 3.9 ppm (C(7)-H); δ 4.3 ppm (C(6)-H); δ 7.2-7.6 ppm (Aromatic protons); δ 9.4 ppm (N-H). ¹³C NMR data (in dimethylsulfoxide-d₆): δ 28.36 ppm (C3-4); δ 58.31 ppm (C2-5); δ 72.30 ppm (C6); δ 87.97 ppm (C7); δ 132.82 ppm (C15-17); δ 133.38 ppm (C14-18); δ 144.84 ppm (C13); δ 156.98 ppm (C10); δ 169.00 ppm (C8-12).

2.3. Inhibition Efficiency (I.E %) Measurements

2.3.1. Weight Loss Measurements

The cleaned and dry specimens were weighed before immersing in 1.0 M hydrochloric acid with and without addition of Mannich base at 300 K for 2 h immersion time without bubbling. In order to investigate the effect of temperature, time, acid concentration and inhibitor, the experiments were carried out at different temperature range of 300-330K, time duration of 2-5 hours, 1-4 M and 100-400 ppm. After a particular immersion time, mild steel specimens were drawn out and rinsed with double distilled water, washed with acetone, dried and weighed. The duplicate experiments were carried out and average values were noted.

The I.E calculated according to the following equation:^[13]

$$I.E(\%) = \frac{W_0 - W}{W_0} \times 100 \quad (1)$$

Where W₀, W are the weight of mild steel before and after immersed in inhibitor solution.

2.3.2. Potentiodynamic Polarization Measurements

Potentiodynamic polarization measurements were performed using an instrument ELECTROCHEMICAL ANALYZER model CH604 B. A three electrode system was adopted for the investigation. The working mild steel electrode embedded in araldite with exposed area 1 cm²; a saturated calomel electrode (SCE) and platinum electrode were used as the reference and counter electrode respectively. The inhibition efficiency was calculated from the following equation.^[14]

$$I.E(\%) = \frac{I'_{corr} - I_{corr}}{I'_{corr}} \times 100 \quad (2)$$

Where I'corr and I_{corr} were corrosion current densities obtained in uninhibited and inhibited solution.

2.3.3. Electrochemical Impedance Spectroscopy (EIS)

Impedance measurement were carried out in the range of 10 KHz to 10 μHz, at the rest potential by applying 5 mV sine wave ac voltage. The same cell and the system as in the polarization method were used. The double layer capacitance (Cdl), charge transfer resistance (R_{ct}) was calculated from Nyquist plots as described. R_{ct} is inversely proportional to corrosion current density; it was used to determine the inhibition efficiency I.E (%) from the relationship.^[15]

$$I.E(\%) = \frac{R'_{ct}}{R'_{ct} - R_{ct}} \times 100 \quad (3)$$

Where R'ct and R_{ct} are the charge resistance values in uninhibited and inhibited solutions.

2.3.4. UV-Visible and FT-IR Studies

UV-visible spectrophotometer experiments were carried out for pure PPMPT and PPMPT after absorbed on mild steel in 1 M HCl. After 4 h immersion of mild steel in a mixture of 1 M HCl and 400 ppm of inhibitor, the mild steel removed and dried. Then the mild steel surface was scrapped with knife to collect the compound absorbed on the mild steel surface. The samples collected were tested by using UV-Visible (PG INSTRUMENT modelT90+) and FT-IR (Perkin Elmer FT-IR instrument).

2.3.5. SEM and EDS Analysis

The specimens used for surface morphology examination were initially immersed in 1.0 M HCl containing 400 ppm of PPMPT for 2 h. Then they removed and rinsed quickly with acetone, dried at room temperature. The morphology analyses were performed on a HITACHI SU6600 scanning electron microscope with an INCA energy X-ray spectrometer.

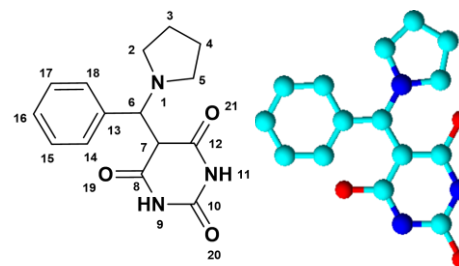


Fig. 1. Molecular structure of 5-(Phenyl-pyrrolidin-1-yl-methyl)-pyrimidine-2,4,6-trione (PPMPT).

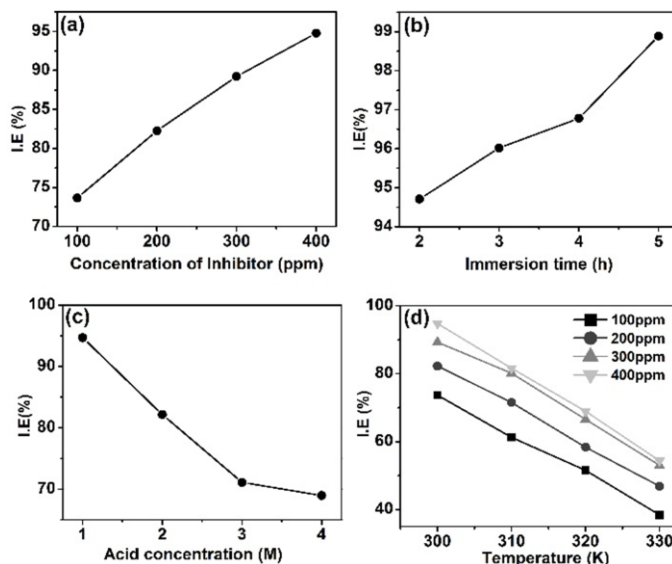


Fig. 2. a) Variation of inhibition efficiency with different inhibitor concentration. b) Variation of inhibition efficiency with different immersion time. c) Variation of inhibition efficiency with different acid concentration. d) Effect of temperature on inhibition efficiency.

3. Results and Discussions

3.1. Weight Loss and Adsorption Isotherms

The corrosion rates and inhibition efficiency obtained from weight loss method at different PPMPPT concentration at 300 K displayed in Fig. 2a. The results show that the synthesized PPMPPT inhibitor effectively inhibits the corrosion of mild steel in HCl medium. It was noticed that the I.E % increase with the inhibitor concentration. This might be due to the increase in the number of inhibitor molecules that could effectively cover the mild steel surface.^[16] The effect of inhibition efficiency at different immersion time was studied. As shown in Fig. 2b, the inhibition efficiency increases from 94% to 99% with increasing immersion time from 2 h to 24 h. This is attributed to the increased adsorption rate with respect to time domain. The variation of inhibition efficiency with change in the acid concentration (from 1.0 M to 4.0 M) has shown in Fig. 2c. The decrease in the inhibition efficiency with increase in acid concentration is mainly due to high aggressiveness of the test solution. The role of temperature on inhibition efficiency was investigated and the results are presented in Fig. 2d. The increase in temperature from 300K to 330K increases the corrosion rate (Fig. 2d) in both inhibited and uninhibited solution. This believed to be increased temperature and their associated H₂ gas evolution in acid media usually accelerates the corrosion reaction, resulting in higher dissolution rate of the metal.^[17] Weakening of adsorbed film on the mild steel surface upon higher temperature should also be a reason for such inhibition decrement. These results confirm that the Mannich bases inhibitor (PPMPPT) is an effective corrosion inhibitor in acid solution up to 330K.

The degree of surface coverage for different concentration of inhibitor at different temperature was evaluated by weight loss measurements. The plot of C/θ against C has been drawn using different temperature and straight lines were obtained. For the inhibitor at 300K, 310K, and 320K, the straight line with slope values of 0.954, 1.8752 and 1.2658 were obtained, respectively. Fig. 3 indicates that the inhibitor obeys Langmuir adsorption isotherm.

Langmuir adsorption isotherm:^[18]

$$\frac{C_{inh}}{\theta} = \frac{1}{K} + C_{inh} \quad (4)$$

Where C_{inh} is the molar concentration of inhibitor, k_{ads} is equilibrium constant. This was calculated by Eq 4.

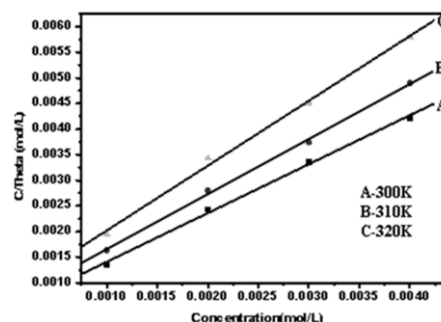


Fig. 3. Langmuir plot for inhibitor on mild steel in 1.0 M HCl.

The most important thermodynamic parameters such as ΔG_{ads} , ΔH_{ads} and ΔS_{ads} are found according to the equations.^[19]

$$\Delta G_{ads} = -RT (\ln 55.5 k_{ads}) \quad (5)$$

Where 55.5 is the molar concentration of water in the solution. The negative value of ΔG_{ads} indicates that spontaneous adsorption of the inhibitor molecule on the metal surface. ΔG_{ads} (around -30 kJ mol⁻¹) reveals that inhibitor can be a mixed type inhibitor (both physisorption and chemisorption) in acid solution.

The enthalpy of activation can be obtained from the following equation:^[20]

$$Rate = \frac{RT}{Nh} \exp \frac{\Delta S}{R} \exp \frac{-\Delta H}{RT} \quad (6)$$

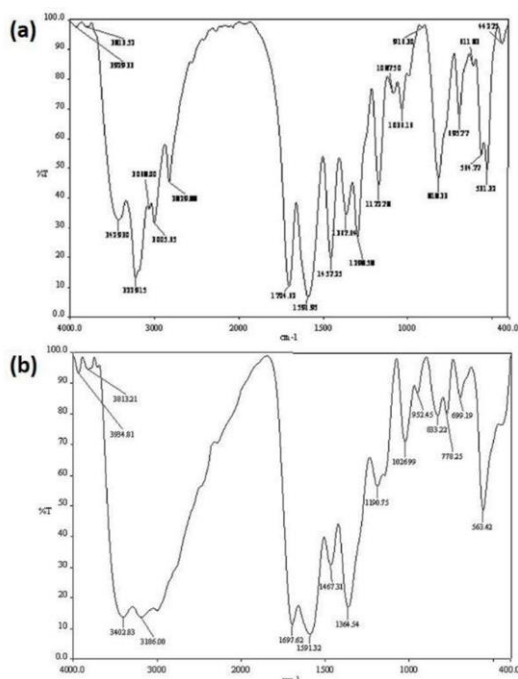
Where h is the Planck's constant, N -Avogadro number and R is the general gas constant.

Table 1. Thermodynamic parameters for the adsorption of PPMPPT molecules on mild steel surface in 1.0 M HCl at different temperatures

Temperature (K)	R ²	Slope	ΔG_{ads} (kJ/mol)	K_{abs} (kJ/mol)	ΔH_{ads} (kJ/mol)	ΔS_{ads} (J K ⁻¹ mol ⁻¹)
300	0.9986	0.954	-29.20	2.197×10^3	-20.22	-30.00
310	0.9992	1.8752	-29.55	1.719×10^3	-20.22	-30.00
320	0.9982	1.2658	-29.80	1.322×10^3	-20.22	-30.00

Table 2. Polarization parameters for the mild steel in 1.0 M HCl at different concentrations of PPMPPT

Concentration Of (ppm)	I_{corr} ($\mu A cm^{-2}$)	E_{corr} (mv)	β_c (mV decade ⁻¹)	β_a (mV decade ⁻¹)	I.E (%)
Blank	659.18	531	4.032	5.764	-
100	46.19	478	5.680	1.303	92.99
200	25.30	491	8.014	1.045	96.16
300	21.53	485	8.190	1.221	96.73
400	21.45	487	8.310	1.220	96.75

**Fig. 4.** (a) FT-IR spectrum of the (b) FT-IR spectrum of adsorbed on metal surface.

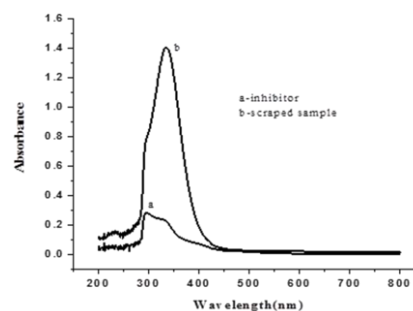
A plot of C/θ and C gave a straight line with the slope of $\Delta H/2.303R$. The enthalpy of activation obtained from the slope shown in the Table 1. The value of ΔH_{ads} is lower which indicates that form a low energy barrier which exhibits high inhibition efficiency at elevated temperature.

ΔS_{ads} was found by the equation given below;^[21]

$$\Delta G_{ads} = \Delta H_{ads} + T \Delta S_{ads} \quad (7)$$

In Table 1, the value of ΔS_{ads} is found to be negative. This indicates that the activated complex in the rate determining step represents an association rather than dissociation step, meaning that a decrease in the disordering from reactant to the activated complex.

FT-IR was recorded to understand the interaction of the molecule with metal surface. Fig. 4a shows the FTIR spectrum of pure sample and Fig. 4b depicts the FTIR spectrum of scraped sample obtained from the metal surface. After corrosion experiments, the peaks of scraped sample were noticed to be significantly modified when

**Fig. 5.** UV-Visible spectrum of inhibitor and scraped sample.

compared to pure PPMPPT. This may be due to the metal-inhibitor binding and Fe-oxide/PPMPPT interaction; stretching frequencies of scraped samples changed.^[22]

The UV-visible absorption spectrum of the solution containing 400 ppm of PPMPPT was recorded. The band at 296 nm is responsible for π to π^* . The PPMPPT coated with mild steel surface were scraped out after 24 h and tested. UV-Visible spectrum of scraped sample (Fig. 5) demonstrates a remarkable band shift at 296 nm (from 296 nm to 334 nm) when compared to pure PPMPPT. The UV-Visible result agrees well with the FT-IR results. Moreover, the formation of Fe-inhibitor complex was also confirmed by the UV-Visible result. It can be noticed that an increase in the absorption (hyperchromic shift) for scraped sample which shows the formation of Fe-inhibitor complex.^[23]

3.2. Electrochemical Measurements

Potentiodynamic polarization curves of mild steel in 1.0 M hydrochloric acid in the absence and presence of inhibitor at room temperature are shown in Fig. 6a. Polarization parameters such as corrosion potential (E_{corr}), cathodic, anodic Tafel slopes and corrosion current density (I_{corr}) were obtained by extrapolation of the Tafel lines and the calculated I.E (%) values are given in Table 2. The maximum I.E of 96% was obtained for the mild steel corrosion at the concentration of 400 ppm of PPMPPT. Higher inhibition efficiency is probably due to presence of heteroatom and aromatic rings.^[24] The inhibition efficiency data Table 2 and Fig. 6a showed that the inhibitor molecules have good interaction with mild steel surface.

Electrochemical impedance measurement was carried out in 1.0 M hydrochloric acid solutions with and without PPMPPT inhibitor. As

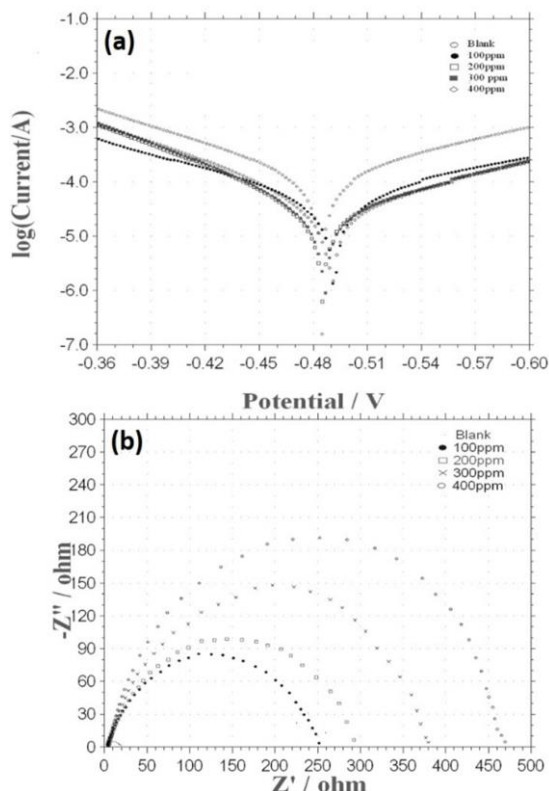


Fig. 6. a) Potentiodynamic polarization curves, b) Impedance analysis of mild steel with different inhibitor concentration. For comparison electrochemical test of blank also measured.

shown in Fig. 6b, the higher frequency region capacitive loop noticed for the mild steel immersed in inhibited solution is mainly due to charge transfer process.^[25] The difference between the intercept at higher frequencies end (R_s) and intercept at lower frequencies end ($R_s + R_{ct}$) gives charge transfer value (R_{ct}). The results show that the R_{ct} value increases with the concentration of PPMPT. The electrochemical impedance parameters derived from the Nyquist plots and the efficiency (I.E %) derived from the same are presented

Table 3. Electrochemical parameters for mild steel in 1M Hydrochloric acid with different concentration of PPMPT.

Concentration of Inhibitor (ppm)	R_{ct} ($\Omega \text{ Cm}^2$)	C_{dl} ($\mu\text{F Cm}^2$)	I.E (%)
100	246.85	20.0	93.44
200	296.79	24.6	94.54
300	391.78	26.5	95.87
400	466.541	28.1	96.53
Blank	16.19	239.6	-

in Table 3. The results obtained from the electrochemical impedance method can be interpreted in terms of equivalent circuit of the double layer shown in Fig. 6b which has been used previously to model the iron/acid interface. The semicircle depends upon the concentration of the PPMPT used in 1 M HCl solution. It can be seen that the diameter of the capacitive loop increases with the concentration of inhibitor PPMPT. The Nyquist plots obtained in the real system represent the double layer on the inner face of metal /solution does not behave as real capacitor on the metal, and control the charge distribution, where as in solution it was controlled by the ions. As ions are much larger than electrons,^[26] the equivalent ions to the charge on the metal will occupy a quite large volume on the solution side of the double layer. From the Table 3, it was clear that the charge transfer resistance values increased with concentration of PPMPT. However, the capacitance values were found to be decreased with increasing concentration. Decreases in the capacitance decreases in the local dielectric constant and increases in the thickness of the double layer. It suggests that the molecules act as adsorbent at metal/solution interface, which form film on the mild steel surface.^[27]

3.3. Surface Analysis

SEM and EDS analysis were performed for the mild steel specimens after immersion in 1.0 M hydrochloric acid solution for 2h with and without addition of inhibitor. The morphology of specimen surface is

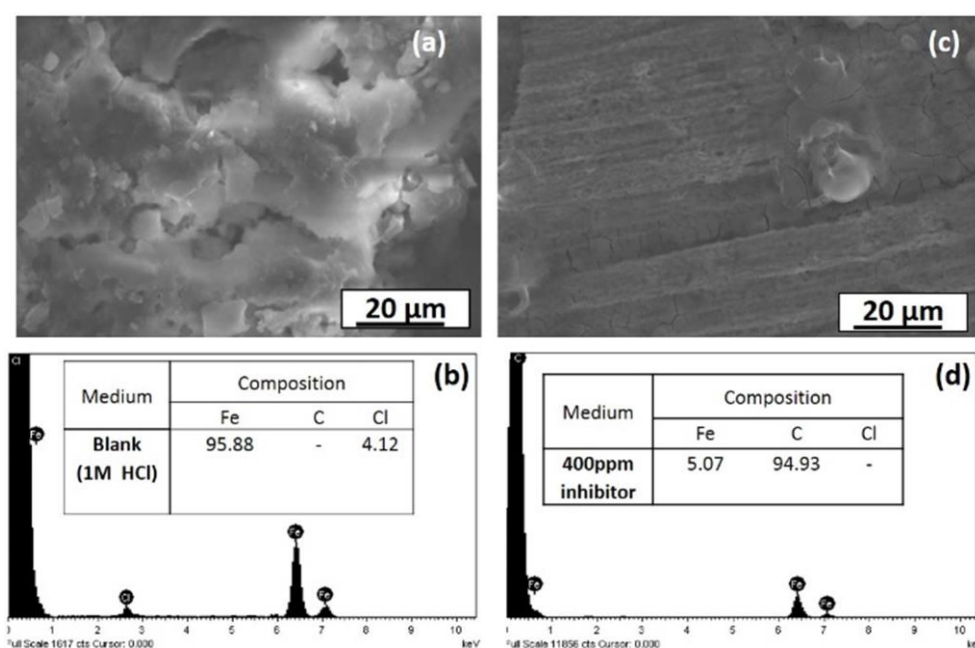


Fig. 7. SEM and EDX image of mild steel immersed in 1 M HCl in (a, b) absence of and (c, d) presence of inhibitor.

shown in Fig. 7a. The SEM image of mild steel confirms that the mild steel surface is severely damaged due to the aggressiveness of the HCl solution.^[28] In Fig.7b, the EDS spectrum showed corrosion product that contain high Cl content (3.12 wt%) with Fe. To our delight, after the addition of inhibitor, the morphology of the mild steel surface becomes smooth without any cracks (Fig. 7). In addition, the EDS spectrum of mild steel after immersion in inhibited solution (Fig. 7d) showed no chlorine content. This is mainly due to the strong production of mild steel by the PPMPT molecules.^[29]

4. Conclusions

5-(Phenyl-pyrrolidin-1-yl-methyl)-pyrimidine-2,4,6-trione compound was confirmed by spectral analysis such as ¹H NMR, ¹³C NMR, FT-IR. When increasing the concentration of inhibitor, the inhibition efficiency increased and obtained maximum efficiency of 96% 400ppm. Both polarization studies and impedance measurements confirms the inhibiting nature of the inhibitor. Tafel parameters give an idea that the inhibitor is cathodic type in nature. FT-IR and UV-Visible spectra of scrapped sample showed a broad peak and enhanced absorption which is probably due peak at co-ordination site frequencies which was bonded to iron and , d-d transition of co-ordinated iron respectively. SEM image of the inhibited surface shown smooth surface, which further denote the efficacy of the inhibitor. Langmuir details provide evidence for both physisorption and chemisorption. Thermodynamic parameter reveals that the adsorption process of was spontaneous.

Conflicts of Interest

The authors declare no conflict of interest.

References

- Zheng X.; Gong M.; Li Q.; Guo L. Corrosion Inhibition of Mild Steel in Sulfuric Acid Solution by Loquat (*Eriobotrya japonica* Lindl.) Leaves Extract. *Sci. Rep.*, 2018, **8**, 9140. [[CrossRef](#)]
- Zhang W.; Li H.J.; Wang M.; Wang L.J.; Zhang A.H.; Wu Y.C. Highly Effective Inhibition of Mild Steel Corrosion in HCl Solution by using Pyrido [1,2-a] Benzimidazoles. *New J. Chem.*, 2019, **43**, 413-426. [[CrossRef](#)]
- Kesavan D.; Gopiraman M.; Sulochana N. Green Inhibitors for Corrosion of Metals: A Review. *Chem. Sci. Rev. Lett.*, 2012, **1**, 1-8. [[CrossRef](#)]
- Bentiss F.; Traisnel M.; Lagrenee M. The Substituted 1, 3, 4-Oxadiazoles: A New Class of Corrosion Inhibitors of Mild Steel in Acidic Media. *Corros. Sci.*, 2000, **42**, 127-146. [[CrossRef](#)]
- Mourya P.; Banerjee S.; Singh M.M. Corrosion Inhibition of Mild Steel in Acidic Solution by *Tagetes Erecta* (Marigold Flower) Extract as a Green Inhibitor. *Corros. Sci.*, 2014, **85**, 352-363. [[CrossRef](#)]
- Manokarana G.; Prabakaran M. Evaluation of Antioxidant and Anticorrosion Activities of *Ligularia Fischeri* Plant Extract. *Chem. Sci. Eng. Res.*, 2019, **1**, 16-24. [[CrossRef](#)]
- Baskar R.; Lgaz H.; Salghi R. Heterocyclic Compounds as Corrosion Inhibitors for Mild Steel: A Review. *Chem. Sci. Eng. Res.*, 2019, **1**, 32-54. [[CrossRef](#)]
- Goyal M.; Kumar S.; Bahadur I.; Verma C.; Ebenso E.E. Organic Corrosion Inhibitors for Industrial Cleaning of Ferrous and Non-Ferrous Metals in Acidic Solutions: A Review. *J. Mol. Liq.*, 2018, **256**, 565-573. [[CrossRef](#)]
- Singh A.; Talha M.; Xu X.; Sun Z.; Lin Y. Heterocyclic Corrosion Inhibitors for J55 Steel in a Sweet Corrosive Medium. *ACS Omega*, 2017, **2**, 8177-8186. [[CrossRef](#)]
- Quraishi M.A.; Khan M.W.; Ajmal M.; Muralidharan S.; Iyer S.V. Influence of Heterocyclic Anils on Corrosion Inhibition and Hydrogen Permeation through Mild Steel in Acid Chloride Environments. *Corrosion*, 1997, **53**, 475-480. [[CrossRef](#)]
- Jeeva M.; Prabhu G.V.; Boobalan M.S.; Rajesh C.M. Interactions and Inhibition Effect of Urea-Derived Mannich Bases on a Mild Steel Surface in HCl. *J. Phys. Chem. C*, 2015, **119**, 22025-22043. [[CrossRef](#)]
- Thiraviyam P.; Kannan K. A Study of Synthesized Mannich Base Inhibition on Mild Steel Corrosion in Acid Medium. *J. Iran. Chem. Soc.*, 2012, **9**, 911-921. [[CrossRef](#)]
- Gopiraman M.; Selvakumaran N.; Kesavan D.; Karvembu R. Adsorption and Corrosion Inhibition Behaviour of N-(phenylcarbamothioyl) Benzamide on Mild Steel in Acidic Medium. *Prog. Org. Coat.*, 2012, **73**, 104-111. [[CrossRef](#)]
- Prabakaran M.; Kim S.H.; Hemapriya V.; Gopiraman M.; Kim I.S.; Chung I.M. *Rhus Verniciflua* as a Green Corrosion Inhibitor for Mild Steel in 1 M H₂SO₄. *RSC Adv.*, 2016, **6**, 57144-57153. [[CrossRef](#)]
- Gopiraman M.; Selvakumaran N.; Kesavan D.; Kim I.S.; Karvembu R. Chemical and Physical Interactions of 1-benzoyl-3, 3-disubstituted Thiourea Derivatives on Mild Steel Surface: Corrosion Inhibition in Acidic Media. *Ind. Eng. Chem. Res.*, 2012, **51**, 7910-7922. [[CrossRef](#)]
- Kumar S.L.A.; Gopiraman M.; Kumar M.S.; Sreekanth A. 2-Acetylpyridine-N (4)-morpholine thiosemicarbazone (HAcPMTSc) as a Corrosion Inhibitor on Mild Steel in HCl. *Ind. Eng. Chem. Res.*, 2011, **50**, 7824-7832. [[CrossRef](#)]
- Rajeswari V.; Kesavan D.; Gopiraman M.; Viswanathamurthi P. Physicochemical Studies of Glucose, Gellan Gum, and Hydroxypropyl Cellulose—Inhibition of Cast Iron Corrosion. *Carbohydr. Polym.*, 2013, **95**, 288-294. [[CrossRef](#)]
- Mert B.D.; Mert M.E.; Kardaş G.; Yazıcı B. Experimental and Theoretical Investigation of 3-amino-1, 2, 4-triazole-5-thiol as a Corrosion Inhibitor for Carbon Steel in HCl Medium. *Corros. Sci.*, 2011, **53**, 4265-4272. [[CrossRef](#)]
- Ji G.; Anjum S.; Sundaram S.; Prakash R. *Musa Paradisica* Peel Extract as Green Corrosion Inhibitor for Mild Steel in HCl Solution. *Corros. Sci.*, 2015, **90**, 107-117. [[CrossRef](#)]
- Sathiya Priya A.R.; Muralidharan V.S.; Subramania A. Development of Novel Acidizing Inhibitors for Carbon Steel Corrosion in 15% Boiling Hydrochloric Acid. *Corrosion*, 2008, **64**, 541-552. [[CrossRef](#)]
- Yildiz R. An Electrochemical and Theoretical Evaluation of 4, 6-diamino-2-pyrimidinethiol as a Corrosion Inhibitor for Mild Steel in HCl Solutions. *Corros. Sci.*, 2015, **90**, 544-553. [[CrossRef](#)]
- Prabakaran M.; Kim S.H.; Kalaiselvi K.; Hemapriya V.; Chung I.M. Highly Efficient *Ligularia Fischeri* Green Extract for the Protection Against Corrosion of Mild Steel in Acidic Medium: Electrochemical and Spectroscopic Investigations. *J. Taiwan Inst. Chem. Eng.*, 2016, **59**, 553-562. [[CrossRef](#)]
- Prabakaran M.; Kim S.H.; Oh Y.T.; Raj V.; Chung I.M. Anticorrosion Properties of Momilactone A Isolated from Rice Hulls. *J. Ind. Eng. Chem.*, 2017, **45**, 380-386. [[CrossRef](#)]
- Khan G.; Basirun W.J.; Kazi S.N.; Ahmed P.; Magaji L.; Ahmed S.M.; Khan G.M.; Rehman M.A.; Badry A.B.B.M. Electrochemical Investigation on the Corrosion Inhibition of Mild Steel by Quinazoline Schiff Base Compounds in Hydrochloric Acid Solution. *J. Colloid Interface Sci.*, 2017, **502**, 134-145. [[CrossRef](#)]
- Lgaz H.; Salghi R.; Jodeh S.; Hammouti B. Effect of Clozapine on Inhibition of Mild Steel Corrosion in 1.0 M HCl Medium. *J. Mol. Liq.*, 2017, **225**, 271-280. [[CrossRef](#)]
- Solmaz R. Investigation of Adsorption and Corrosion Inhibition of Mild Steel in Hydrochloric Acid Solution by 5-(4-Dimethylaminobenzylidene) Rhodanine. *Corros. Sci.*, 2014, **79**, 169-176. [[CrossRef](#)]
- Kowsari E.; Arman S.Y.; Shahini M.H.; Zandi H.; Ehsani A.; Naderi R.; Pourghasemi-Hanza A.; Mehdipour M. In Situ Synthesis, Electrochemical and Quantum Chemical Analysis of an Amino Acid-Derived Ionic Liquid Inhibitor for Corrosion Protection of Mild Steel in 1M HCl Solution. *Corros. Sci.*, 2016, **112**, 73-85. [[CrossRef](#)]

- 28 Ostovari A.; Hoseinie S.M.; Peikari M.; Shadizadeh S.R.; Hashemi S.J. Corrosion Inhibition of Mild Steel in 1 M HCl Solution by Henna Extract: A Comparative Study of the Inhibition by Henna and its Constituents (Lawson, Gallic acid, α -d-Glucose and Tannic acid). *Corros. Sci.*, 2009, **51**, 1935-1949. [[CrossRef](#)]
- 29 Gopiraman M.; Sakunthala P.; Kesavan D.; Alexramani V.; Kim I.S.; Sulochana N. An Investigation of Mild Carbon Steel Corrosion Inhibition in Hydrochloric Acid Medium by Environment Friendly Green Inhibitors. *J. Coat. Technol. Res.*, 2012, **9**, 15-26. [[CrossRef](#)]



© 2020, by the authors. Licensee Ariviyal Publishing, India. This article is an open access article distributed under the terms and conditions of the Creative Commons Attribution (CC BY) license (<http://creativecommons.org/licenses/by/4.0/>).